



A two-decades (1988-2009) record of diatom fluxes in the Mauritanian coastal upwelling:
Impact of low-frequency forcing and a two-step shift in the species composition

3

Oscar E. Romero^{1, 2,*}, Simon Ramondenc^{1,2} and Gerhard Fischer^{1,3}

6

¹MARUM – Center for Marine Environmental Sciences, University of Bremen, Leobener Str. 8, 28359
Bremen, Germany

9

²Alfred Wegener Institute, Helmholtz Centre for Polar and Marine Research, 27568 Bremerhaven,
Germany

³University of Bremen, Geosciences Department, Klagenfurter Str., 28359 Bremen, Germany

*E-mail corresponding author: oromero@marum.de; oromero@uni-bremen.de

12

Key words: coastal upwelling, decadal, diatoms, Eastern Boundary Upwelling Ecosystems, fluxes,
Mauritania, multiyear, northwest Africa, sediment traps, time-series

15

Abstract

18

Eastern Boundary Upwelling Ecosystems (EBUEs) are among the most productive marine regions in
the world's oceans. Understanding the degree of interannual to decadal variability in the Mauritanian
upwelling system is key for the prediction of future changes of primary productivity and carbon
sequestration in the Canary Current EBUE as well as in similar environments. A multiannual sediment
trap experiment was conducted at the mooring site CBmeso (= 'Cape Blanc mesotrophic', ca. 20°N, ca.
20°40'W) in the high-productive Mauritanian coastal waters. Here, we present results on fluxes and
the species-specific composition of the diatom assemblage for the time interval between March 1988
and May 2009. The temporal dynamics of diatom populations allows to propose three main diatom
productivity/flux intervals: (i) early 1988 - late 1996; (ii) 1997 - 1999, and (iii) early 2002 - mid 2009.
The impact of the Atlantic Multidecadal Oscillation appears to be an important forcing of the long-
term dynamics of diatom population. The impact of cold (1988-1996) and warm AMO phases (2001-
2009) is reflected by the outstanding shifts in species-specific composition. This AMO-impacted, long-
term trend is interrupted by the occurrence of the strong 1997 ENSO. The extraordinary shift in the
relative abundance of benthic diatoms in May 2002 suggests the strengthening of offshore advective
transport within the uppermost layer of filament waters, and in the subsurface and in deeper and
bottom-near layers. It is hypothesized that the dominance of benthic diatoms was the response of
the diatom community to the intensification of the slope and shelf poleward undercurrents. This
dominance followed the intensification of the warm phase of AMO and the associated changes of the
Atlantic Meridional Overturning Circulation. Transported valves (siliceous remains) from shallow
coastal waters into the deeper bathypelagial should be considered for the calculation and model

33



36 experiments of bathy- and pelagial nutrients budgets (especially Si), the burial of diatoms and the
paleoenvironmental signal preserved in downcore sediments. Our 1988-2009 data set contributes to
the distinction between climate-forced and intrinsic variability of populations of diatoms and will be
39 especially helpful for establishing the scientific basis for forecasting and modelling future states of
this ecosystem and its decadal changes.

42 **1 Introduction**

As part of the latitudinally extended Eastern Boundary Upwelling Ecosystem (EBUE) of the Canary
Current (CC) in the subtropical northeastern Atlantic, the Mauritanian upwelling is characterized by
45 intense offshore Ekman transport and strong mesoscale heterogeneity. This physical setting
facilitates the vigorous exchange between the neritic and pelagic realms off Mauritania (Chavez and
Messié, 2009; Cropper et al., 2014; Freón et al., 2009). The nutrient trapping efficiency of upwelling
48 cells (Aristegui et al., 2009), the input of wind-carried dust particles from the Sahara and the Sahel
(Fischer et al., 2016; Fischer et al., 2019; Friese et al., 2016; Romero et al., 1999, 2003), and/or the
wide shelf (Hagen, 2001; Cropper et al., 2014) additionally impact the intensity of the primary
51 production in surface waters and the subsequent export of microorganism remains into the
bathypelagial off Mauritania. This set of conditions varies strongly on different temporal patterns
(from seasonal through decadal; Mittelstaedt, 1983, 1991; Hagen, 2001; Nykjær and Van Camp,
54 1994; Barton et al., 2013; Varela et al., 2015). Whether the strong interannual and decadal variability
of physical conditions off Mauritania is related to low frequency, global-scale climatic variations or to
an intrinsic level of basin-wide atmospheric and/or oceanic variability is still a matter of debate
57 (Cropper et al., 2014, Fischer et al., 2016, 2019; Varela et al., 2015).

EBUEs may prove more resilient to on-going climate change than other ocean ecosystems
because of their ability to function under extremely variable conditions (Barton et al., 2013; Varela et
60 al., 2015). On the other hand, it is predicted that current global warming will impact atmospheric
pressure gradients and hence the strength of coastal winds that cause upwelling (Bakun, 1990; Bakun
et al., 2013). Although productivity variations in EBUEs are sensitive to the amplitude and timing of
63 upwelling-favorable winds (Varela et al., 2015), the impact of on-going ocean warming on the
dynamics of upwelling-favorable winds is still contentious (Bakun, 1990; Bakun et al., 2013; Varela et
al., 2015). Long-term trends in variations of upwelling intensity and related productivity changes
66 seem highly dependent on the length of the data series, the selected study area, the season
evaluated, and the methods applied (Varela et al., 2015). The description of multiyear to interdecadal
trends of upwelling intensity in the CC-EBUE has been mostly based on variations of velocity and
69 direction of winds and calculated upwelling intensities. Cropper et al. (2014) found a non-significant
increase in upwelling-favorable winds along the CC-EBUE between 11° and 35°N. Using the same



72 database as Cropper et al. (2014), Narayan et al. (2010) and Patti et al. (2011) analyzed the annual
wind stress over four decades and found significant increasing trends across 24°–32°N. Contradictory
73 results were also obtained using Ekman transport data. Gómez-Gesteira et al. (2008) detected a
significant decreasing trend in upwelling intensity across 20°–32°N for all seasons between 1967 and
74 2006, while Pardo et al. (2011) found a general weakening of upwelling intensity between 10 and
24°N for the time interval 1970–2009. Barton et al. (2013) found no statistically significant change of
the annual mean wind intensity off Northwest Africa over the second half of the 20th century.

75
76
77
78 A different approach for the characterization of multiyear to interdecadal trends in EBUEs is
assessing fluxes of particulates and microorganisms as captured by continuous sediment trap
experiments. This study builds on earlier investigations of multiyear variability of the diatom flux
79 captured with sediment traps deployed at the mesopelagial mooring site CBmeso (= ‘Cape Blanc
mesotrophic’, formerly known as CB, Fig. 1; Fischer et al., 1996). Several earlier studies addressed
80 either the variations of total diatom fluxes between 03/1988 and 11/1991 (Lange et al., 1998;
Romero et al., 1999a, 2002; Romero and Armand, 2010) or the land-derived signal of siliceous
81 remains (Romero et al., 1999b, 2003). After a gap of 2,5 years (12/91 through 05/94), the CBmeso
trap experiment re-started in June 1994 (Table 1). Here, we extend the diatom record collected from
82 early June 1994 until middle June 2009. The main goal of this study is the description of the multiyear
dynamics of the total diatom flux (TDF) and the shifts in the species-specific composition of the
83 assemblage at site CBmeso during almost 20 years (1988–2009). To our knowledge, our study
presents the longest sediment trap-based time-series on the temporal dynamics of diatom fluxes in a
84 low-latitude EBUE. We discuss the new results in view of the high-frequency atmospheric and
hydrographic dynamics along the CC-EBUE, and low-frequency climate variability in the North
85 Atlantic, and compare our new dataset at site CBmeso with previous diatom (Romero and Fischer,
2017; Lange et al., 1998; Romero et al., 1999a,b; 2002, 2020), as well as bulk flux results off
86 Mauritania (Fischer et al., 2016, 2019; Helmke et al., 2005). We also discuss our new results with
recent results from the near-by, coastal site CBeu (= ‘Cape Blanc eutrophic’) (Romero and Fischer,
87 2017; Romero et al., 2020).

98 2 Material and Methods

99 2.1 Mooring location, sampling intervals and sample treatment

A total of 20 moorings were deployed off Mauritania (ca. 21°N, 20°W, Fig. 1) between March 1988
and May 2009. Details on sampling intervals and trap depths are given in Table 1. Major gaps in the
100 diatom record are between: (i) December 1991 and June 1994 (no traps deployed), (ii) October 1994
and November 1995 (malfunctioning of the trap CBmeso6 upper); (iii) October 1997 and June 1998
(malfunctioning of the trap CBmeso8 upper), and November 1999 and March 2001 (malfunctioning
101 of traps CBmeso10 and 11 lower) (Table 1).
102
103
104
105



We used deep-moored (>1000 m depth), large-aperture, time-series sediment traps of the Kiel and Honjo types with 20 cups and 0.5 m² openings, equipped with a honeycomb baffle (Kremling et al., 1996). As the traps were moored in deep waters (mostly below 1,200m, Table 1), uncertainties with the trapping efficiency due to strong currents (*e.g.* undersampling) and/or due to the migration and activity of zooplankton migrators ('swimmer problem') are assumed to be minimal (Buesseler et al., 2007). Prior to the deployments, the sampling cups were poisoned with HgCl₂ (1 ml of conc. HgCl₂ per 100ml of filtered seawater) and pure NaCl was used to increase the density in the sampling cups to 40‰. Upon recovery, samples were stored at 4°C on board and wet-split in the home laboratory (MARUM, University of Bremen) using a rotating McLane wet splitter system. Larger swimmers –such as crustaceans– were handpicked at the home lab by using forceps and were removed by filtering carefully through a 1 mm sieve. All flux data here refer to the size fraction <1 mm. In almost all samples, the fraction of particles >1 mm was negligible, only in a few samples larger pteropods were found (Fischer et al., 2016).

We compare our data with those previously published at the mooring location CBeu (ca. 20°45'N, 18°45'W), also deployed off Mauritania (Romero and Fischer, 2017; Romero et al., 2020). It locates ca. 80 nautical miles (~150 km) offshore over the continental slope in ca. 2,750 m water depth. For site CBeu, only the upper trap fluxes are shown (Romero and Fischer, 2017; Fischer et al., 2019; Romero et al., 2020).

2.2 Assessment of diatom fluxes and species identification

1/64 and 1/125 splits of the original samples were used. Samples were rinsed with distilled water and prepared for diatom studies following standard methods (Schrader and Gersonde, 1978). For this study, a total of 282 sediment trap samples was processed. Each sample was chemically treated with potassium permanganate, hydrogen peroxide (33%) and concentrated hydrochloric acid (32%) following previously used methodology (Romero and Fischer, 2017; Romero et al., 1999a, b, 2002, 2009a, b; 2020). Qualitative and quantitative analyses of the diatom community were carried out on permanent slides of acid cleaned material (*Mountex*[®] mounting medium) at x1000 magnifications by using a *Zeiss*[®] Axioscop with phase-contrast illumination (MARUM, University of Bremen). Depending on valve abundances in each sample, several traverses across each slide were examined. The counting procedure and definition of counting units for valves follows Schrader and Gersonde (1978). Total amount of counted valves per slide ranged between ca. 400 and 1,000. Two cover slips per sample were scanned in this way. Counts of valves in replicate slides indicate that the analytical error of valve concentration estimates is ≤10 %.

The resulting counts yielded abundance of individual diatom taxa as well as daily fluxes of valves per m⁻² d⁻¹ (DF), calculated according to Sancetta and Calvert (1988), as follows:

$$DF = \frac{[N] \times [A/a] \times [V] \times [Split]}{}$$



[days] x [D]

where, [N] number of valves in a known area [a], as a fraction of the total area of a petri dish [A]
141 and the dilution volume [V] in ml. This value is multiplied by the sample split [Split], representing the
fraction of total material in the trap, and then divided by the number of [days] of sample deployment
and the sediment trap collection area [D].

144 2.3 Statistical analysis

Correspondence Analysis (CA) was used to explore diatoms community's changes. CA is an
ordination technique that enables describing the community structure from multivariate contingency
147 tables with frequency-like data (*i.e.* abundances derived from counting with integers and zeros) that
are dimensionally homogeneous (Legendre and Legendre, 2012). Based on the CA samples' scores, a
hierarchical clustering analysis was performed to classify the samples date according to the diatom
150 composition similarities. Euclidean distance was used to compute the distance matrix from which a
hierarchical dendrogram was generated using Ward's aggregation link (Legendre and Legendre,
2012). This approach has been computed by using the *vegan* package included in the R software. In
153 addition, Kruskal Wallis tests, coupled with multiple comparison tests (pairwise Wilcoxon rank sum
test) have been performed on climatic indexes and TDF according to sample groups highlighted by
the clustering analysis with the aim of identifying relationships between environmental forcing
156 indices and diatom communities.

3 Physical setting of the study area

159 3.1 Oceanography, winds, and upwelling dynamics

The CC-EBUE is in the eastern part of the North Atlantic subtropical gyre (Fig. 1; Arístegui et al.,
2009; Chavez and Messié, 2009; Cropper et al., 2014). Both the temporal occurrence and the
162 intensity of the upwelling along northwestern Africa depend on the shelf width, the seafloor
topography, wind direction and strength (Mittelstaedt, 1983; Hagen, 2001), the Ekman-mediated
transport and strong mesoscale heterogeneity (Chavez and Messié, 2009; Cropper et al., 2014; Fréon
165 et al., 2009). The Mauritanian shelf is wider than the shelf northward and southward along the CC-
EBUE and gently slopes from the coastline into water depths below 200 m (Hagen, 2001). The shelf
break zone with its steep continental slope extends over approximately 100 km from the coastline
168 (Hagen, 2001). As a consequence of the coastal topography, and the shelf and slope bathymetry, the
ocean currents and the wind system, surface waters off Mauritania are characterized by almost
permanent upwelling with varying intensity year-through (Lathuilière et al., 2008; Cropper et al.,
171 2014). Site CBmeso locates at the westward end of this permanent upwelling zone.

The surface hydrography off Mauritania is strongly influenced by two surface currents: the
southwestward-flowing CC and the poleward-flowing coastal countercurrent or Mauritania Current



174 (MC) (Fig. 1). The surficial CC detaches from the northern African continental slope between 25° and
21°N and supplies Si-poor waters to the North Equatorial Current. CC waters are relatively cool
because it entrains upwelled water from the coast as it moves southward (Mittelstaedt, 1991). The
177 Si-rich MC gradually flows northward along the coast up to about 20°N (Mittelstaedt, 1991), and
brings warmer surface waters from the equatorial realm into waters overlying site CBmeso. Towards
late autumn, the MC is gradually replaced by a southward flow associated with upwelling water due
180 to the increasing influence of trade winds south of 20°N (Zenk et al., 1991), and becomes a narrow
strip of less than 100 km width in winter (Mittelstaedt, 1983). The MC advances onto the shelf in
summer and is enhanced by the relatively strong Equatorial Countercurrent and the southerly trade
183 winds (Mittelstaedt, 1983).

North of Cape Blanc (ca. 21°N; Fig. 1), the intense northeasterly winds cause coastal upwelling to
move further offshore and the upper slope fills with upwelled waters. South of Cape Blanc, northerly
186 winds dominate year-through, but surface waters remain stratified and the coastal Poleward
Undercurrent (PUC) occurs as a subsurface current (Pelegrí et al., 2017). South of Cape Timiris (ca.
19°30'N), the PUC intensifies during summer-fall and remains at the subsurface during winter-spring
189 (Pelegrí et al., 2017). The encountering of the northward flowing MC-PUC system with the southward
flowing currents builds the Cape Verde Frontal Zone (Zenk et al., 1991; Fig. 1) and the large offshore
water export is visible as the giant Mauritanian chlorophyll filament (Gabric, 1993; Pelegrí et al.,
192 2006, 2017).

The chlorophyll filament extends offshore up to 400 km (*e.g.*, Arístegui et al., 2009; Cropper et al.,
2014; Van Camp et al., 1991), carrying a mixture of North and South Atlantic Central Water (NACW
195 and SACW, respectively) through an intense jet-like flow offshore (Meunier et al., 2012). Intense
offshore transport acts an important mechanism for the export of cool, nutrient-rich shelf and upper
slope waters. It has been estimated that this giant filament export about 50% of the coastal new
198 production offshore toward the open ocean during intervals of most intense upwelling (Gabric et al.,
1993; Helmke et al., 2005; Lange et al., 1998; Van Camp et al., 1991). This transport impacts even
more distant regions in the deep ocean, since sinking particles are strongly advected by lateral
201 transport in subsurface and deeper waters (Fischer and Karakaş, 2009; Fischer et al., 2009; Karakaş et
al., 2006).

The SACW occurs in layers between 100 and 400 m depth the Banc d'Arguin and off Mauritania.
204 The hydrographic properties of upwelled waters over the shelf suggest that they ascend from depths
between 100 and 200 m south off the Banc d'Arguin (Mittelstaedt, 1983). North of it, the SACW
merges gradually into deeper layers (200-400 m) below the CC (Mittelstaedt, 1983). The biological
207 response is drastically accelerated in upwelled waters when the SACW of the upper part of the
undercurrent feeds the onshore transport of intermediate layers to form mixed-water types on the



shelf (Zenk et al., 1991).

210 **3.2 Large-scale, low-frequency climate and oceanographic modes potentially affecting the**
211 **Mauritanian upwelling area**

212 **3.2.1 Atlantic Multidecadal Oscillation (AMO):** is the average of sea surface temperatures (SST) of
213 the North Atlantic Ocean (from 0° to 60°N, 80°W to 0°), detrended to isolate the natural variability
(Endfield et al., 2001). It is an on-going series of multidecadal cyclicity, with cool and warm phases
216 that may last 20-40 years at a time with a difference of about 15°C between extremes. These
changes are natural and have been occurring for at least the last 1,000 years. Since AMO is linked to
SST variations, it also plays a significant role in the decadal forcing of productivity changes (O'Reilly et
al., 2016). Fischer et al. (2016) state that the correlation of sea-level pressure with area-averaged (0–
219 70°N, 60–10°W) SST fluctuations over periods longer than 10 years highlights a center of action in the
tropical Atlantic with sea-level pressure reductions (weaker northeasterly winds) along with higher
Atlantic basin-wide sea-level pressure during a positive AMO phase. This shows the importance of
222 longer-term, Atlantic basin-scale SST variations for alongshore winds and upwelling trends at site
CBmeso.

223 Despite the indirect role for the atmosphere, the physical connection between the Atlantic
225 Meridional Overturning Circulation (AMOC) and the AMO is typically described in terms of oceanic
processes alone: since the AMOC transports heat northward over the entire Atlantic, an increase in
NADW formation should increase the strength of the AMOC, thus increasing oceanic meridional heat
228 transport convergence in the North Atlantic, resulting in a basin-scale warming of SSTs (Knight et al.,
2005). Atlantic Meridional Overturning Circulation (AMOC) variability itself is often attributed to
changes in North Atlantic Deep Water (NADW) formation due to anomalous Arctic freshwater fluxes
231 (Jungclaus et al., 2005) and/or atmospheric modes such as the North Atlantic Oscillation (*e.g.*,
Buckley and Marshall, 2016). In contrast, Clement et al. (2015) found that the pattern of AMO
variability can be reproduced in a model that does not include ocean circulation changes, but only
234 the effects of changes in air temperature and winds.

235 **3.2.2 El Niño/Southern Oscillation (ENSO) and La Niña:** is an irregularly periodic variation in winds
237 and SST over the tropical eastern Pacific Ocean, affecting the climate of much of the tropics and
subtropics of other ocean basins. The warming phase is known as El Niño and the cooling phase as La
Niña. The Southern Oscillation is the accompanying atmospheric component, coupled with the SST
variations. ENSO-related teleconnections in the CC-EBUE upwelling system have been described by
240 several authors (Behrenfeld et al., 2001; Pradhan et al, 2006; Zeeberg et al., 2008) and can be
illustrated by the negative correlation of sea level pressure with eastern tropical Pacific SST.

241 **3.2.3 North Atlantic Oscillation (NAO):** characterizes the difference of atmospheric sea level
243 pressure between the Icelandic Low and the Azores High (Hurrell, 1995). These fluctuations control



the strength and direction of westerly winds and location of storm tracks across the North Atlantic. It varies over time with no periodicity. A positive phase of the NAO is associated with anomalous high pressure in the Azores high region and stronger northeasterly winds along the NW African coast. Especially during the months of November through April, the NAO is responsible for much of the variability of weather in the North Atlantic region, affecting wind speed and wind direction changes, changes in temperature and moisture distribution and the intensity, number and track of storms. Correlations during winter show that NAO and ENSO may have opposite effects on the CC-EBUE/northeastern Atlantic realm, for instance on wind fields, and consequently on upwelling with potential implications for deep ocean mass fluxes (Fischer et al., 2016).

4 Results

4.1 Total diatom fluxes

Marine diatoms are the main contributors to the siliceous fraction in samples collected with the CBmeso traps between March 1988 and June 2009. Silicoflagellates and radiolarians are secondary components of the siliceous fraction (not shown here), with minor contribution of land-derived freshwater diatoms and phytoliths. In term of number of individuals, the TDF was always one order to four orders of magnitude higher than that of the other siliceous organisms.

The TDF ranged 2.7×10^3 – 3.3×10^6 valves $\text{m}^{-2} \text{d}^{-1}$ (average = 4.0×10^5 valves $\pm 4.4 \times 10^5$), and shows strong interannual variability (Fig. 2). Highest fluxes ($>1.0 \times 10^6$ valves $\text{m}^{-2} \text{d}^{-1}$) occurred in 1988, late 1989, early 2002, 2003, late 2004, early 2005, early 2007 and early 2008. The lowest total diatom flux was recorded between 1997 and 1999 (range = 2.3×10^3 – 5.1×10^4).

Maxima of TDF are defined here as those values that are higher than the TDF average ± 1 standard deviation (STD) for the entire study period. Spring and summer show the higher amount of above-the-average TDF. Although the same number of maxima are recorded in fall as in summer and spring (n=17; spring, n=16), the absolute values of fall TDF maxima were predominantly lower than those of spring and summer. Winter has the lowest amount of TDF maxima (n=12).

4.2 Temporal variations of marine diatom populations

A total of 203 diatom species were identified in CBmeso samples between March 1988 and June 2009. To better understand the temporal variations of the diverse community, we follow the same grouping approach as already applied in the nearby trap site CBeu (Romero and Fischer, 2017; Romero et al., 2020). Out of 203 taxa, 109 species (whose average relative contribution is $\geq 0.50\%$ for the entire studied interval) were distributed in four groups, according to the main ecological and/or habitat conditions they represent: (1) benthic, (2) coastal upwelling, (3) coastal planktonic, and (4) open-ocean diatoms. Taxa assigned to each group are listed in Table 2. Below the main species of each group and their main ecological significance are shortly described.



279 (1) The benthic group is dominated by *Delphineis surirella*. As part of the epipsammic
community, *D. surirella* is a benthic marine species that commonly thrives in the shallow euphotic
282 zone of sandy shores, shelf and uppermost slope waters along temperate to cool seas, forming either
short or long chains of small valves (length=5-15 μm) (Andrews, 1981).

(2) The coastal upwelling group is composed by several species of *Chaetoceros* resting spores
(RS) and the vegetative cells of *Thalassionema nitzschioides* var. *nitzschioides*. Both taxa are common
285 components of the coastal and hemipelagial upwelling assemblages in EBUes (Romero and Armand,
2010; Abrantes et al., 2002; Nave et al., 2001; Romero et al., 2002). Vegetative cells of numerous
Chaetoceros species (mainly those assigned to the section *Hyalochaete*, Rines and Hargraves, 1988)
288 rapidly respond to the weakening of upwelling intensity and nutrient depletion by forming
endogenous resting spores, hence their high numbers in trap samples is interpreted to represent the
strongest upwelling intensity (Romero and Armand, 2010; Abrantes et al., 2002; Nave et al., 2001;
291 Romero et al., 2002).

(3) Coastal planktonic species mostly thrive in neritic to hemipelagic, oligo-to-mesotrophic
waters with moderate levels of dissolved silica (DSi). These species become more abundant during
294 intervals of decreased mixing, when upwelling weakens (Romero and Armand, 2010; Romero and
Fischer, 2017; Crosta et al., 2012; Romero et al., 2009a; Romero et al., 2009b; Romero et al., 2020).
The well-silicified species *Actinocyclus curvatulus*, *Cyclotella litoralis*, *Coscinodiscus radiatus* and
297 *Shionodiscus oestrupii* var. *venrickae* are the main contributors at the CBmeso site.

(4) Open-ocean taxa thrive in pelagic, oligotrophic, and warm to temperate waters with low
siliceous productivity due to low DSi availability and weak mixing in surface waters (Romero and
300 Fischer, 2017; Nave et al., 2001; Romero et al., 2005; Crosta et al., 2012). This highly diverse group is
dominated by several species of *Azpeitia*, together with *Fragilariopsis doliolus*, *Nitzschia bicapitata*,
Nitzschia interruptestriata, *Roperia tessellata* and *Planktoniella sol*.

303 The multivariate analyses performed on the relative abundance of diatom populations (Fig. 3)
confirms the strong interannual variability with significant shifts within the diatom community
between 1988 and 2009. The first CA component covers 65.47% of the total variance and opposes
306 the samples dominated by benthic and coastal planktonic diatoms (Fig. 3a). The second CA axis
explains 19.16% of the total variance and discriminates coastal upwelling and open ocean diatom. The
clustering analysis allows the samples to be statistically grouped, and the complete time series was
309 segmented according to the four diatoms communities' affiliation (Fig. 3b). These clusters show clear
changes of diatom populations' contribution throughout the time series (Fig. 3c) with the dominance
of open-ocean and coastal upwelling populations between 1988 and 1996. Open-ocean diatoms
312 dominated from 1997 to 2001, while benthic taxa were main contributors from 2002 to 2009.



A major shift in the relative contribution of the diatom groups is seen from May 2002 onward. This shift occurred in two steps (Fig. 2b). The percentage of benthic diatoms strongly increased
315 between middle May/early June 2002 (raise from 12.5 to 68.6%; trap CBmeso13, samples 2 and 3). Benthic diatom contribution decreased below 40% in early 2004. A second increase occurred in
318 winter 2006, with values being mostly above 50% almost throughout until the end of the trap experiment in June 2009 (Fig. 2b). The dominance of benthic diatoms at CBmeso also prevails after 2009 (Oscar E. Romero, unpublished data). The marked increase of variability of the benthic relative contribution is clearly evidenced by the highest variability among all diatom groups (1STD of each
321 group for the entire study is: (1) benthic = $\pm 23.68\%$, (2) coastal upwelling = $\pm 10.46\%$, (3) coastal planktonic = $\pm 11.88\%$ and (4) open-ocean = $\pm 16.00\%$).

The impact of the environmental variables on diatom communities was investigated by simple
324 comparison using the samples clustering and the forcing values associated (Fig 4). AMO, the Shannon diversity index and TDF show significant differences between groups (Kruskall-Wallis test; p -
327 $value < 0.05$) whereas no statistical differences have been observed for the NAO, ENSO and Pacific Decadal Oscillation indices. Only benthic diatoms (group 4) shown higher AMO values compared to the three other groups (pairwise Wilcoxon rank sum test; p -
330 $value < 0.05$). In addition, a Shannon diversity index gradient has been mainly observed with low, intermediate and high values in samples dominate by benthic (*i.e.* group 4), coastal planktonic (*i.e.* group 3) and coastal upwelling/open-
333 ocean (*i.e.* group 2/1) populations, respectively (pairwise Wilcoxon rank sum test; p -
336 $value < 0.05$). The statistical analysis also highlights that, during the dominance of the coastal upwelling populations, the TDF was higher compared to TDF when other diatom group/s dominated the community. The correlogram performed between CA axes and the low-frequency climate indices also confirms these trends (not shown here). A significant positive and negative correlation has been found between the
339 first CA axis samples scores' with respectively AMO and Shannon diversity index (Fig. 3). Given that the first CA is positively driven by the benthic group, this confirms that the outstanding dominance of the benthic diatom *D. surirella* decreased the diversity, although it also seems to be promoted by AMO strengthening. In the same way, the second CA axis samples scores are positively correlated with TDF, which confirms that coastal upwelling diatoms seems to promote the TDF.

342 5 Discussion

The long-term diatom record at site CBmeso offers the possibility of discussing population
345 dynamics in the context of the high-frequency atmospheric and hydrographic dynamics along the CC-EBUE, and low-frequency climate variability such in the North Atlantic. In 5.1, we discuss the impact of climate forcing on the long-term trends of the diatom community and the TDF, and the two-step shift in the species-specific composition of diatom populations. In the second subsection, we



348 compare the CBmeso data with those previously published at the hemipelagic site CBeu (Romero and
Fischer, 2017; Romero et al., 2020), and discuss (i) the effect of the giant chlorophyll filament and (ii)
the impact of lateral advection from the coastal area off Mauritania upon the hemi- and pelagial
351 along the NE Atlantic Ocean.

Based on outstanding shifts in the species-specific composition of the diatom assemblage
occurred throughout the study interval (Fig. 2b). We propose three main intervals in the multiyear
354 evolution of populations and discuss them in view of major environmental forcings: (i) early 1988 -
late 1996 (gradually decreasing trend of coastal upwelling diatoms); (ii) 1997–1999 (highest
contribution of open-ocean diatoms); and (iii) 2002–middle 2009 (major shift in the species-specific
357 composition: extraordinary increase and dominance of benthic diatoms).

5.1 The impact of low frequency forcing on the variability of diatom populations off Mauritania

5.1.1 AMO and the two-step increase of benthic diatoms' contribution

360 Based on the long-term trends of our data and their statistical analysis (Figs. 2-5), we suggest that
the proposed intervals were the response of the diatom populations to the impact of low frequency
forcing. As described above in 4.2, the benthic diatom community appears positively correlated with
363 AMO (Fig. 5). Among the low frequency forcings affecting the subtropical North Atlantic (see above
3.2), the AMO plays a key role in determining decadal variations of SST and meridional circulation
(e.g., Knight et al., 2005; Wang and Zhang, 2013; McCarthy et al., 2015). It is widely accepted that
366 AMO is largely induced by AMOC variations and the associated fluctuations of heat transport
(Medhaug and Furevik, 2011; Wang and Zhang, 2013; Knight et al., 2005; McCarthy et al., 2015;
details in 3.2.1). Using observational data and model experiments, Wang and Zhang (2013) conclude
369 that the cooling of the subtropical North Atlantic (where the CBmeso is deployed) towards the end of
the warm AMO phase is largely due to the meridional advection by the anomalous northward
current. The anomalous cooling appears below 100 m and extend down to ca. 1,500 m water depth,
372 with a maximum cooling around 200 m between 8° and 20°N. During the cold phase of the AMO, the
anomalous southward meridional current is responsible for the subsurface ocean warming (Wang
and Zhang, 2013).

375 An additional effect of the AMO impact is the significant long-term weakening (strengthening) of
the gyre during warm (cold) phase of AMO. This weakening contributes to the anomalous northward
current in the subsurface (ca. 100-200 m), while its strengthening causes the anomalous southward
378 current. The decrease of upwelling diatoms' contribution between 1988 and 1996 (Fig. 2b) matches
the transition from a predominantly cool into a warm AMO phase during the late 1990s (Fig. 5; Wang
and Zhang, 2013, and references therein). The simultaneous increase in the contribution of open-
381 ocean diatoms is additional evidence for decreased diatom productivity (Fig. 2) and the predominant



occurrence of oligo-mesotrophic waters bathing the CBmeso site towards the earliest 1990s, with the stronger input of the silica-depleted NACW (see 3.1).

384 An extraordinary feature of the multiyear dynamics of diatom populations at the CBmeso site is
the sharp shift in the species contribution (Fig. 2b). Linked to the intensification of the warm AMO
387 phase into the latest 1990s, the anomalous northward MC strengthened the advection into open
waters (Wang and Zhang, 2013). These physical setting might have led to a stronger input of the DSi-
rich SACW. The MC mixes into the giant Mauritanian chlorophyll filament and, thus, positively
390 impacts diatom productivity by supplying DSi also during summer and fall, far earlier than the
typically wind-induced upwelling off Mauritania (mainly occurring in late winter-early spring,
Mittelstaedt, 1983; Cropper et al., 2014).

The species shift into larger contribution of benthic diatoms follows a two-step increase pattern:
393 the first abrupt increase is observed in late May/early June 2002. The second increase occurs in
winter 2006, with values mostly above 50% almost until the end of the trap experiment (June 2009,
Fig. 4). The dominance of benthic taxa also prevails after afterward throughout until recently
396 recovered traps at site CBmeso (Oscar E. Romero, unpublished data). As already observed in previous
studies at the more neritic site CBeu (Romero and Fischer, 2017; Romero et al., 2020; see further
discussion in 5.2), the diatom *D. surirella* also dominates the benthic community at site CBmeso.
399 Since this small diatom (length=5-15 μm) mostly occurs attached to sand grains in shallow marine
habitats within the euphotic zone and is occasional component of the thycoplanktonic community
(Andrews, 1981), they originally thrive in shallow waters (above 50m depth) overlying the wide
402 Mauritanian upper shelf, are suspended and transported downslope until reaching the traps at the
bathypelagial CBmeso site.

The intensification of the transport of AMOC intermediate waters during the warm phase of the
405 AMO (Wang and Zhang, 2013) might have also contributed to the strengthening of lateral transport
from subsurface shelf waters upon the hemi- and bathypelagial off Mauritania. Earlier studies at the
CBmeso time-series (Fischer et al., 2009, 2016) and observation-based model experiments conducted
408 along the Mauritanian upwelling (Helmke et al., 2005; Karakaş et al., 2006; Nowald et al., 2015)
discussed already the role of intermediate and deep nepheloid layers in the lateral transport of
particles and microorganisms remains upon the deeper bathypelagial. Based on the vigorous mixing
411 in the uppermost water column due to the confluence of northward and southward water masses
and strong, predominantly westward winds off Mauritania (Fig. 1; see 3.1), the offshore transport
from shallow into deeper waters is most intense between 20.5°N and 23.5°N along the northwestern
414 African margin. Erosional processes in the very dynamic coastal realm significantly contribute to the
downward transport of particulates and microorganism remains (Meunier et al., 2012), and are
responsible for sporadic particle clouds advected up to several hundreds of kilometers offshore



417 within intermediate and bottom-near nepheloid layers (Fischer and Karakaş, 2009; Fischer et al.,
2009, Nowald et al., 2015). This nepheloid layer-mediated transport additionally benefits from the
420 bathymetry of the Mauritanian shelf and slope (Nowald et al., 2015). The subsurface layer (100 to
300 m water depth), in turn strongly affected by the AMOC intensification due to AMO impact (Wang
and Zhang, 2013), might be the place of mixing processes of laterally-advected materials from the
423 shelf (where benthic diatoms predominantly thrive) by the activity of the giant chlorophyll filament,
with relatively fresh material derived from the open ocean surface (as represented by the other
three diatom groups). As the nepheloid layer-mediated transport contribute more intensively to the
426 deposition of diatom remains upon the lower slope and beyond than the direct vertical settling from
euphotic layer does after 2001, the area of final burial of diatom valves is effectively displaced from
their production area in surface waters overlying the CBmeso site into their area of final deposition in
deep-sea sediments below 4,000 m water depth.

429 **5.1.2 The occurrence of the strong 1997 ENSO and the response of the diatom community off Mauritania**

432 The long-term trends determined by the cold and warm phases of AMO was altered in the second
half of the 1990s by the impact of the strong 1997 ENSO (McPhaden, 1999). Although caution is
advised in the interpretation of the record due to a few gaps between 1996 and 1999 (Table 1), we
435 postulate that both low coastal upwelling diatom values ($\leq 4\%$) and TDF between February 1997
and November 1999 (Fig. 2b) are the response of the diatom community to the impact of ENSO upon
the low-latitude NW Atlantic. The dominance of taxa predominantly related to waters of low-to-
moderate productivity (1997: highest contribution of open-ocean diatoms and lowest of coastal
438 upwelling diatoms; 1998-99: highest contribution of coastal planktonic and open-ocean diatoms,
typical of oligo-mesotrophic waters) evidences considerable changes in the physical setting of the
Mauritanian upwelling. Since the interval 1996-1999 records the lowest TDF for the entire study (Fig.
441 2a), we argue that ENSO negatively impacted on diatom productivity off Mauritania and most of the
total organic carbon captured with CBmeso traps (Fischer et al., 2016), was instead delivered either
by coccolithophorids or bacterioplankton.

444 A positive ENSO goes along with the weakening of E-NE winds off Mauritania (Pradhan et al.,
2006; Fischer et al., 2016). Weakened E-NE trades lead to the deepening of the thermocline below
the depth of the source of upwelled water, this hindering the mixing of the water column and
447 causing upwelling intensity off Mauritania to decrease until early 1998 (Pradhan et al., 2006).
Additionally, the size of the Mauritanian chlorophyll filament decreased between winter 1997 and
spring 1998, while became unusually large from autumn 1998 to spring 1999 (Fischer et al., 2009).
450 Aperiodic, pronounced decreases in the diatom flux in other ocean basins have been previously
associated with limiting nutrient levels due to ENSO-derived perturbations. The diatom production in



hemipelagial waters off northern Chile decreased extraordinarily during the strong 1997 ENSO compared to earlier years (Romero et al., 2001). Similar negative impact assigned to ENSO teleconnections have been observed in the California Current (Lange et al., 2000), in the Cariaco Basin (Romero et al., 2009b) and in the pelagial Subarctic Pacific Ocean (Takahashi, 1987).

Complementary support of this ENSO-mediated impact on surface water productivity off Mauritania is provided by variations of bulk biogenic fluxes at CBmeso. The almost 2.5 times higher organic carbon flux during 1998-99 than in 1997 (Helmke et al., 2005) led to propose that, after weakening due to impact of ENSO on the physical setting, upwelling intensified immediately afterward during La Niña (Fischer et al., 2016). Similarly, the seasonal cycle of surface Chl-*a* distribution in waters above the CBmeso site reveals a noticeable event (~250% increase) in Mauritanian coastal waters (Pradhan et al., 2006).

5.2 Comparison of diatom fluxes and populations' dynamics within the giant Mauritanian chlorophyll filament (CBmeso vs CBeu)

In this subsection, we compare the diatom flux and the assemblage composition at site CBmeso with previous results from the nearby trap site CBeu gained between 2003 and 2009 (Romero and Fischer, 2017; Romero et al., 2020). The CBeu site locates ca. 80 nautical miles (~150 km) offshore at the continental slope below the giant Mauritanian chlorophyll filament, and hence between the coastline and the outer CBmeso site (Fig. 1). These two trap locations are under different nutrient availability and upwelling intensity between eutrophic (CBeu) and mesotrophic conditions (CBmeso) (Romero and Fischer, 2017; Fischer et al., 2016, 2019).

The less favorable conditions for diatom productivity in waters overlying site CBmeso is evidenced by lower TDF than at site CBeu. On the seasonal pattern, TDF at site CBmeso are always two orders of magnitude lower than values gained at site CBeu (Fig. 6a). This also happens during fall, when the highest average seasonal flux is recorded at CBmeso ($5.6 \cdot 10^5$ valves $m^{-2} d^{-1}$ vs $3.3 \cdot 10^6$ valves $m^{-2} d^{-1}$). We advocate that these flux differences reflect (i) the offshore weakening of the transport via the chlorophyll filament, (ii) the seaward decreasing concentration of nutrients within the filament (Lathuilière et al., 2008; Meunier et al., 2012), (iii) the more intense upwelling in waters overlying the Mauritanian slope (Mittelstaedt, 1983, 1991; Cropper et al., 2014), and (iv) the offshore weakening of the lateral transport (Karakas et al., 2006; Nowald et al., 2015). According to satellite imagery (Van Camp et al., 1991; Gabric et al., 1993; Fischer et al., 2016), the CBmeso mooring locates only occasionally beneath the giant chlorophyll filament and hence below nutrient-rich waters. In general, the larger DSi availability (approximately 10 vs. 5 μM) and the higher Si:N ratios of the source waters (SACW vs. NACW = 0.6 vs. 0.3; Arístegui et al., 2009) in coastal waters bathing site CBeu are reflected in ca. threefold higher BSi fluxes at the coastal CBeu -whose fluxes are additionally affected by



486 stronger ballasting due to higher lithogenic input from northwestern Africa- compared to the
487 offshore CBmeso (Fischer et al., 2019).

489 Complementary support to the scenario of lower (higher) productivity levels at CBmeso (CBeu) is
490 provided by the species-specific composition of the assemblage: relative contribution of groups
491 related with more oligo-mesotrophic waters is higher at CBmeso than at CBeu (coastal planktonic
492 and open-ocean, Fig. 6d, e), while the opposite is true for diatoms typical of eutrophic waters (Fig.
493 6c). Despite the difference in the relative contribution, the species-specific composition of diatom
494 groups is remarkably similar at both sites. All the main group taxa at site CBmeso (Table 2, see also
495 4.2) are also found in CBeu samples (see Table 2 in Romero and Fischer, 2017). This match makes
496 sense as both trap sites are linked via lateral advection through near-surface, intermediate and
497 deeper nepheloid layers. In their earlier study, Romero and Fischer (2017) observed that the shift in
498 the species composition at site CBeu toward a benthic-dominated assemblage occurred in early
499 winter 2006. Since benthic diatoms in the deeper CBmeso traps are transported via nepheloid layers
500 from shallow coastal waters (see 5.1.1), the high percentage of benthic species at the CBmeso site
501 (Fig. 6b) also evidences the impact of particulates derived from the Mauritanian inner shallow shelf
502 (Romero and Fischer, 2017; Fischer et al., 2009, 2016, 2019; Romero et al., 2020). The simultaneous
503 occurrence of the second increase of benthic diatoms at CBmeso and the increase at the neritic site
504 CBeu (Fig. 5) is a striking feature of the population shift over a large part of the Mauritanian
505 upwelling system. The transport of particulates and microorganism remains from their source in
506 shallow coastal waters into the hemipelagic realm probably occurs within weeks (Karakaş et al.,
507 2006, 2009). Phytoplankton thriving in Mauritanian surface waters can be transported as far as 400
508 km offshore from coastal waters (Gabric et al., 1993; Helmke et al., 2005; Barton et al., 2013). The
509 MC might have helped in detaching benthic diatoms from their substrata (Romero and Fischer, 2017)
510 and in transporting them northwestward into the hemipelagic/bathypelagic realm (where CBmeso
511 traps are deployed). These observations offer additional evidence of the impact of AMO via the
512 strengthening of the meridional advection, the major nutrient input via the MC and the nepheloid
513 layer-mediated transport into the deeper Mauritanian bathypelagic.

513 6 Conclusions

514 This multiyear diatom study offers an overall picture of the long-term evolution of diatom-based
515 productivity and fluxes and the response of diatom populations to the interaction of high- and low-
516 frequency hydrographic and atmospheric forcing in the mid-latitude NE Atlantic Ocean. A unique,
517 persistent trend in the long-term evolution of the TDF, either decreasing or increasing, is not
518 recognized in our ca. 20-year record.
519



522 The statistical analysis supports the proposed scenario of AMO as an important driver of diatom
populations' dynamics off Mauritania. The correspondence of cold (1988-1996) and warm AMO
525 phases (2001-2009) is reflected by the shift in species-specific composition. This overall trend is
interrupted by the occurrence of the strong 1997 ENSO. Changes in the physical setting following
1997 ENSO (weakening of E-NE trade winds, thermocline deepening, weakened water column
531 mixing) negatively impacted diatom fluxes off Mauritania.

Our CBmeso trap results allow corroborating that the abrupt shift in the assemblage composition
occurred earlier off Mauritania (starting May 2002) than previously demonstrated (Romero and
528 Fischer, 2017; Romero et al., 2020) and followed two steps. The two-step increase of benthic
diatoms at the CBmeso site suggests that the intensification of the slope and shelf poleward
undercurrents followed the intensification of the warm phase of AMO and the associated AMOC
531 changes.

Diatom remains sink not only vertically off Mauritania, but they are also laterally advected from the
shelf to the deeper bathypelagial via the nepheloid layer-mediated transport. Transported valves
534 (siliceous remains) from shallow coastal waters into the deeper bathypelagial should be considered
for the calculation and model experiments of bathy- and pelagial nutrients budgets (especially Si),
the burial of diatoms and the paleoenvironmental signal preserved in downcore sediments.

537 Understanding the degree of interannual to decadal variability in the Mauritania upwelling system is
key for the prediction of future changes of primary productivity along the NW African margin as
well in other, economically important EBUes. Our 1988-2009 data set might be instrumental in
540 distinguishing between climate-forced and intrinsic variability of populations of primary producers
(*e.g.*, diatoms) and are especially important for establishing the scientific basis for forecasting and
modeling future states of this ecosystem and its decadal changes.

543

Code and Data Availability

Data are available at <https://doi.pangaea.de/10.1594/PANGAEA.921237>

546

Author Contributions

OER and GF devised the study. OER collected the data and wrote the manuscript. SR performed
549 the statistical analysis. All authors contributed to interpretation and discussion of results.

Competing Interests



552 The authors declare that they have no conflict of interest.

Acknowledgements

555 We are greatly indebted to the masters and crews of the RVs Meteor, MS Merian, Polarstern and
Poseidon for several research expeditions along off Mauritania. Much appreciated is the help of the
RV Poseidon headquarters at Geomar (Klas Lackschewitz, Kiel, Germany) during the planning phases
558 of these research expeditions and the support by the German, Moroccan and Mauritanian
governments. The Institut Mauretaniien de Recherches Océanographiques et des Pêches at
Nouadhibou (Mauritania) is acknowledged for its support and help in getting the necessary
561 permissions to perform our multiyear trap experiments in Mauritanian coastal waters. Götz Ruhland,
Nico Nowald and Marco Klann (MARUM, Bremen) were responsible for the mooring deployments
and home lab work. The long-term funding by the German Research Foundation (DFG) through SFB
564 261, the Research Center Ocean Margins (RCOM) and the current MARUM Excellence Cluster “The
Ocean in the Earth System” (University of Bremen, Bremen, Germany) made this study possible.



567 **References**

- 570 Abrantes, F., Meggers, H., Nave, S., Bollman, J., Palma, S., Sprengel, C., Henderiks, J., Spies, A., Salgueiro, E., Moita, T., and Neuer, S.: Fluxes of micro-organisms along a productivity gradient in the Canary Islands region (29°N): implications for paleoreconstructions, *Deep-Sea Res. II*, 49, 3599–3629, 2002.
- Andrews, G. W.: Revision of the diatom genus *Delphineis* and morphology of *Delphineis surirella* (Ehrenberg) G. W. Andrews, n. comb, edited by: Ross, R., *Proc. Sixth Diatom Symp.*, Otto Koeltz, Koenigstein, 81–92, 1981.
- 573 Arístegui, J., Barton, E.C., Álvarez-Salgado, X.A., Santos, A.M.P., Figueiras, F.G., Kifani, S., Hernández-León, S., Mason, E., Machú, E., and Demarcq, H., Sub-regional ecosystem variability in the canary current upwelling, *Prog. Oceanogr.*, 83, 33–48, doi:10.1016/j.pocean.2009.07.031, 2009.
- 576 Bakun, A.: Global climate change and intensification of coastal ocean upwelling, *Science*, 247, 198–201, 1990.
- Barton, E.D., Field, D.B., and Roy, C.: Canary current upwelling: More or less, *Prog. Oceanogr.*, 116, 167–178, 2013.
- 579 Behrenfeld, M. J., Randerson, J.T., McClain, C.R., Feldman, G.C., Los, S.O., Tucker, C.J., Falkowski, P.G., Field, C.B., Frouin, R., Esaias, W.E., Kolber, D.D., and Pollack, N.H.: Biospheric Primary Production During an ENSO Transition, *Science*, 291, 2594–2597, 2001.
- 582 Buckley, M.W., and Marshall, J.: Observations, inferences, and mechanisms of Atlantic Meridional Overturning Circulation variability, *Rev. Geophys.*, 54, 5–63, doi:10.1002/2015RG000493, 2016.
- 585 Buesseler, K.O., Antia, A.A., Chen, M., Fowler, S.W., Gardner, W.D., Gustafsson, O., Harada, K., Michaels, A.F., Rutgers van der Loeff, M., Sarin, M., Steinberg, D.K., and Trull, T.: An assessment of the use of sediment traps for estimating upper ocean particle fluxes, *J. Mar. Res.*, 65, 345–416, 2007.
- 588 Chavez, F.P., and Messié, M.: A comparison of Eastern Boundary Upwelling Ecosystems, *Prog. Oceanogr.*, 83, 80–96, 2009.
- Clement, A., Bellomo, K., Murphy, L.N., Cane, M.A., Mauritsen, T., Rädcl, G., and Stevens, B.: The Atlantic Multidecadal Oscillation without a role for ocean circulation, *Science*, 350(6258), 320–324, doi:10.1126/science.aab3980, 2015.
- 591 Cropper, T. E., Hanna, E., and Bigg, G.R.: Spatial and temporal seasonal trends in coastal upwelling off Northwest Africa, 1981–2012, *Deep-Sea Res. I*, 86, 94–111, 2014.
- 594 Crosta, X., Romero, O. E., Ther, O., and Schneider, R. R.: Climatically-controlled siliceous productivity in the eastern Gulf of Guinea during the last 4000yr, *Clim. Past*, 8, 415–431, <https://doi.org/10.5194/cp-8-415-2012>, 2012.
- 597 Enfield, D. B., Mestas-Nuñez, A.M., and Trimble, P.J.: The Atlantic Multidecadal Oscillation and its relation to rainfall and river flows in the continental U.S., *Geophys. Res. Lett.*, 28(10), 2077–2080, 2001.
- 600 Fischer, G. and Karakaş, G.: Sinking rates and ballast composition of particles in the Atlantic Ocean: implications for the organic carbon fluxes to the deep ocean, *Biogeosciences*, 6, 85–102, <https://doi.org/10.5194/bg-6-85-2009>, 2009.
- 603 Fischer, G., Reuter, C., Karakaş, G., Nowald, N., and Wefer, G.: Offshore advection of particles within the Cape Blanc filament, Mauritania: Results from observational and modelling studies, *Prog. Oceanogr.* 83, 322–330, 2009.
- 606 Fischer, G., Romero, O., Merkel, U., Donner, B., Iversen, M., Nowald, N., Ratmeyer, V., Ruhland, G., Klann, M., and Wefer, G.: Deep ocean mass fluxes in the coastal up- welling off Mauritania from 1988 to 2012: variability on seasonal to decadal timescales, *Biogeosciences*, 13, 3071–3090, <https://doi.org/10.5194/bg-13-3071-2016>, 2016.
- 609 Fischer, G., Romero, O.E., Toby, E., Iversen, M., Donner, B., Mollenhauer, G., Nowald, N., Ruhland, G., Klann, M., Hamady, B., and Wefer, G.: Changes in the Dust-Influenced Biological Carbon Pump in the Canary Current System: Implications From a Coastal and an Offshore Sediment Trap Record Off Cape Blanc, Mauritania, *Global Biogeochem. Cy.*, 33, 1100–1128, 2019.
- 612 Fréon, P., Barange, M., and Arístegui, J.: Eastern Boundary Upwelling Ecosystems: Integrative and comparative approaches. *Prog. Oceanogr.*, 83(1-4), 1–14, <https://doi.org/10.1016/j.pocean.2009.08.001>, 2009.



- 615 Friese, C. A., van Hateren, J. A., Vogt, C., Fischer, G., and Stuu, J.-B.W.: Seasonal provenance changes in present-day Saharan dust collected in and off Mauritania, *Atmos. Chem. Phys.*, **17**, 10163–10193, <https://doi.org/10.5194/acp-17-10163-2017>, 2017.
- 618 Gabric, A. J., Garcia, L., Van Camp, L., Nykjaer, L., Eifler, W. and Schrimpf, W.: Offshore export of shelf production in the Cape Blanc (Mauritania) giant filament as derived from Coastal Zone Color Scanner Imagery, *J. Geophys. Res.*, **98**, 4697-4712, 1993.
- 621 Gómez-Gesteira, M., De Castro, M., Álvarez, I., Lorenzo, M.N., Gesteira, J.L.G., Crespo, A.J.C.: Spatio-temporal Upwelling Trends along the Canary Upwelling System (1967–2006), *Ann. N. Y. Acad. Sci.*, **1146**, 320–337, doi: 10.1196/annals.1446.004, 2008.
- 624 Hagen, E.: Northwest African upwelling scenario, *Oceanol. Acta*, **24**, S113–S128, 2001.
- Hasle, G. A. and Syvertsen, E. E.: Marine diatoms, in: *Identifying marine diatoms and dinoflagellates*, edited by: Thomas, C., Academic Press, Inc. San Diego, CA, 1–385, 1996.
- 627 Helmke, P., Romero, O. E., and Fischer, G.: Northwest African upwelling and its effect on off-shore organic carbon export to the deep sea, *Global Biogeochem. Cycles*, **19**, GB4015, <https://doi.org/10.1029/2004GB002265>, 2005.
- 630 Hurrell, J.W.: Decadal Trends in the North Atlantic Oscillation, *Science*, **269** (5224), 676 679, doi:10.1126/science.269.5224.676, 1995.
- 633 Jungclaus, J. H., Haak, H., Latif, M., and Mikolajewicz, U.: Arctic-North Atlantic interactions and multidecadal variability of the meridional overturning circulation, *J. Climate*, **18**(19), 4013–4031, 2005.
- Karakaş, G., Nowald, N., Blaas, M., Marchesiello, P., Frickenhaus, S., and Schlitzer, R.: High-resolution modeling of sediment erosion and particle transport across the northwest African shelf, *J. Geophys. Res.*, **111**, C06025, doi.org/10.1029/2005JC003296, 2006.
- 636 Karakaş, G., Nowald, N., Schäfer-Neth, C., Iversen, M., Barkmann, W., Fischer, G., Marchesiello, P., and Schlitzer, R.: Impact of particle aggregation on vertical fluxes of organic matter, *Prog. Oceanogr.*, **83**, 331-341, 2009.
- 639 Knight, J.R., Allan, R.J., Folland, C.K., Vellinga, M., and Mann, M.E.: A signature of persistent natural thermohaline circulation cycles in observed climate, *Geophys. Res. Lett.*, **32**, L20708, doi:10.1029/2005GL024233, 2005.
- 642 Kremling, K., Lentz, U., Zeitzschell, B., Schulz-Bull, D.E., and Duinker, J.C.: New type of time-series sediment trap for the reliable collection of inorganic and organic trace chemical substances, *Rev. Sci. Instrum.*, **67**, 4360-4363, 1996.
- 645 Lange, C.B., Romero, O.E., Wefer, G. and Gabric, A.J.: Offshore influence of coastal upwelling off Mauretania, NW Africa, as recorded by diatoms in sediment traps at 2195m water depth, *Deep-Sea Res. I*, **45**, 985-1013, 1998.
- 648 Lange, C.B., Weinheimer, A.L., Reid, F.M.H., Tappa, E. and Thunell, R.C.: Response of siliceous microplankton from the Santa Barbara Basin to the 1997-98 El Niño Event, *Cal. Coop. Ocean. Fish*, **41**, 186-193. 2000
- 651 Lathuilière, C., Echevin, V., and Levy, M.: Seasonal and intraseasonal surface chlorophyll-a variability along the north- west African coast, *J. Geophys. Res.-Oceans*, **13**, C05007, <https://doi.org/10.1029/2007JC004433>, 2008.
- 654 Legendre, P. and Legendre, L.F., 2012, *Numerical ecology*, *Developments in Environmental Modelling*, Vol. 24. Elsevier.
- McCarthy, G. D., Smeed, D. A., Johns, W.E., Frajka-Williams, E., Moat, B.I., Rayner, D., Baringer, M.O., Meinen, C.S., Collins, J., and Bryden, H.J., *Measuring the Atlantic Meridional Overturning Circulation at 26°N*, *Prog. Oceanogr.*, **130**, 91–111, doi:10.1016/j.pocean.2014.10.006, 2015.
- 657 McPhaden, M.J.: Genesis and Evolution of the 1997-98 El Niño, *Science*, **283**, 950-954, 1999.
- 660 Medhaug, I., and Furevik, T.: North Atlantic 20th century multidecadal variability in coupled climate models: sea surface temperature and ocean overturning circulation, *Ocean Sci.*, **7**(3), 389-404 doi:10.5194/os-7-389-2011, 2011.
- 663 Meunier, T., Barton, E.D., Barreiro, B., and Torres, R.: Upwelling filaments off Cape Blanc: interaction of the NW African upwelling current and the Cape Verde frontal zone eddy field?, *J. Geophys. Res.-Oceans*, **117**, C8, C08031, <https://doi.org/10.1029/2012JC007905>, 2012.



- 666 Mittelstaedt, E.: The upwelling area off Northwest Africa – a description of phenomena related to coastal upwelling, *Prog. Oceanogr.*, 12, 307–331, 1983.
- Mittelstaedt, E.: The ocean boundary along the northwest African coast: Circulation and oceanographic properties at the sea surface, *Prog. Oceanogr.*, 26, 307–355, 1991.
- 669 Narayan, N., Paul, A., Mulitza, S., and Schulz, M.: Trends in coastal upwelling intensity during the late 20th century, *Ocean Sci.*, 6, 815–823, 2010.
- 672 Nave, S., Freitas, P., and Abrantes, F.: Coastal upwelling in the Canary Island region: spatial variability reflected by the surface sediment diatom record, *Mar. Micropaleontol.*, 42, 1–23, 2001.
- 675 Nowald, N., Iversen, M. H., Fischer, G., Ratmeyer, V., and Wefer, G.: Time series of in-situ particle properties and sediment trap fluxes in the coastal upwelling filament off Cape Blanc, Mauritania, *Prog. Oceanogr.*, 137, 1–11, 2015.
- Nyckjær, L., and Van Camp, L.: Seasonal and interannual variability of the coastal upwelling along northwest Africa and Portugal from 1981 to 1991, *J. Geophys. Res.*, 99, 14197–14207, 1994.
- 678 O'Reilly, C.H., Huber, L.M., Woollings, T., and Zanna, L.: The signature of low-frequency oceanic forcing in the Atlantic Multidecadal Oscillation, *Geophys. Res. Lett.*, 43(6), 2810–2818, doi 10.1002/2016GL067925, 2016.
- 681 Pardo, P., Padín, X., Gilcoto, M., Farina-Busto, L., and Pérez, F.: Evolution of upwelling systems coupled to the long term variability in sea surface temperature and Ekman transport, *Clim. Res.*, 48, 231–246, 2011.
- 684 Patti, B., Guisande, C., Riveiro, I., Thejll, P., Cuttitta, A., Bonanno, A., Basilone, G., Buscaino, G., and Mazzola, S.: Effect of atmospheric CO₂ and solar activity on wind regime and water column stability in the major global upwelling areas, *Est. Coast. Shelf Sci.*, 88, 45–52, <https://doi.org/10.1016/j.ecss.2010.03.004>, 2010.
- Pelegrí, J.L., Marrero-Díaz, A., and Ratsimandresy, A.W.: Nutrient irrigation of the North Atlantic, *Prog. Oceanogr.*, 70(2–4), 366–406, 2006.
- 687 Pelegrí, J.L., Peña-Izquierdo, J., Machín, F., Meiners, C., and Presas-Navarro, C.: Oceanography of the Cape Verde Basin and Mauritanian Slope Waters, edited by; Ramos, A., et al., *Deep-Sea Ecosystems Off Mauritania*: 119–153, DOI 10.1007/978-94-024-1023-5_3, 2017.
- 690 Pradhan, Y., Lavender, S.J., Hardman-Mountford, N.J., and Aiken, J.: Seasonal and inter-annual variability of chlorophyll-a concentration in the Mauritanian upwelling: Observation of an anomalous event during 1998–1999, *Deep-Sea Res. I*, 53, 1548–1559, 2006.
- 693 Rines, J.E.B., and Hargraves, P.E.: The *Chaetoceros* Ehrenberg (Bacillariophyceae) Flora of Narragansett Bay, Rhode Island, U.S.A, *Bibl. Diatomol.*, 79, 196 pp, 1988.
- 696 Romero, O. E. and Armand, L. K.: Marine diatoms as indicators of modern changes in oceanographic conditions, in: *The Diatoms, Applications for the Environmental and Earth Sciences (Second Edition)*, edited by: Smol, J. P. and Stoermer, E. F., Cambridge University Press, Cambridge, 373–400, 2010.
- 699 Romero, O.E., and Fischer, G.: Shift in the species composition of the diatom community in the eutrophic Mauritanian coastal upwelling: Results from a multi-year sediment trap experiment (2003 – 2010), *Prog. Oceanogr.*, 159, 31–44, 2017.
- 702 Romero, O.E., Lange, C.B., Fischer, G., Treppke, U.F., and Wefer, G.: Variability in export production documented by downward fluxes and species composition of marine planktonic diatoms: Observations from the tropical and equatorial Atlantic, edited by: Fischer, G. und Wefer, G., *The Use of Proxies in Paleoceanography - Examples from the South Atlantic*. Springer Verlag Berlin, Heidelberg, pp. 365–392. 1999a
- 705 Romero, O. E., Lange, C. B., Swap, R.J. and Wefer, G.: Eolian-transported freshwater diatoms and phytoliths across the equatorial Atlantic record temporal changes in Saharan dust transport patterns, *J. Geophys. Res.*, 104, 3211–3222, 1999b.
- 708 Romero, O. E., Hebbeln, D. and Wefer, G.: Temporal and spatial distribution in export production in the SE Pacific Ocean: evidence from siliceous plankton fluxes and surface sediment assemblages, *Deep-Sea Res. I*, 48, 2673–2697, 2001.
- 711 Romero, O. E., Lange, C.B., and Wefer, G.: Interannual variability (1988–1991) of siliceous phytoplankton fluxes off northwest Africa, *J. Plank. Res.* 24(10), 1035–1046. doi:10.1093/plankt/1024.1010.10352002, 2002.
- 714 Romero, O. E., Dupont, L., Wyputt, U., Jahns, S., and G. Wefer, G.: Temporal variability of fluxes of eolian-transported freshwater diatoms, phytoliths, and pollen grains off Cape Blanc as reflection of land-atmosphere-



- ocean interactions in northwest Africa, *J. Geophys. Res.* 108(C5, 3153), doi:10.1029/2000JC000375, 002003, 2003.
- 717 Romero, O. E., Armand, L.K., Crosta, X., and Pichon, J.-J.: The biogeography of major diatom taxa in 2003 Southern Ocean surface sediments: 3. Tropical/Subtropical species, *Palaeogeogr. Palaeoclimatol.*, 223, 49–65, 2005.
- 720 Romero, O. E., Rixen, T., and Herunadi, B.: Effects of hydrographic and climatic forcing on diatom production and export in the tropical southeastern Indian Ocean, *Mar. Ecol. Progr. Ser.*, 384, 69–82, doi: 10.3354/meps08013, 2009a.
- 723 Romero, O. E., Thunell, R.C., Astor, Y., and Varela, R.: Seasonal and interannual dynamics in diatom production in the Cariaco Basin, Venezuela, *Deep-Sea Res. I*, 56(4), 571–581, doi:10.1016/j.dsr.2008.10.102, 2009b.
- 726 Romero, O. E., Baumann, K.-H., Zonneveld, K. A. F., Donner, B., Hefter, J., Hamady, B., Pospelova, V., and Fischer, G.: Flux variability of phyto- and zooplankton communities in the Mauritanian coastal upwelling between 2003 and 2008, *Biogeosciences*, 17(1), 187–214, <https://doi.org/10.5194/bg-5117-5187-2020>, 2020.
- 729 Round, F. E., Crawford, R. M., and Mann, D. G.: *The diatoms*, Cambridge University Press, Cambridge, 747 pp., 1990.
- Sancetta, C. and Calvert, S.E.: The annual cycle of sedimentation in Saanich Inlet, British Columbia: implications for the interpretation of diatom fossil assemblages, *Deep-Sea Res.*, 35, 71–90, 1988.
- 732 Schrader, H.-J. and Gersonde, R.: Diatoms and silicoflagellates, in: *Micropaleontological counting methods and techniques – an exercise on an eight meter section of the Lower Pliocene of Capo Rosello, Sicily*, edited by: Zachariasse, W. J., Riedel, W. R., Sanfilippo, A., Schmidt, R. R., Broolsma, M. J., Schrader, H., Gersonde, R., Drooger, M. M., and Broekman, J. A., *Utrecht Micropaleontological Bulletin*, Utrecht, 17, 129–176, 1978.
- 735 Takahashi, K.: Response of subarctic Pacific diatom fluxes to the 1982–1983 El Niño disturbance, *J. Geophys. Res.*, 93, 14, 387–392, 1987.
- 738 Varela, R. I. Á., Santos, F., de Castro, M., and Gómez-Gesteira, M.: Has upwelling strengthened along worldwide coasts over 1982–2010?, *Scientific Reports*, 5, 10016, DOI: 10.1038/srep10016, 2015.
- 741 Van Camp, L., Nykjær, L., Mittelstaedt, E. and Schlittenhardt, P.: Upwelling and boundary circulation off Northwest Africa as depicted by infrared and visible satellite observations, *Prog. Oceanog.*, 26, 357–402, 1991.
- 744 Wang, C., and Zhang, L.: Multidecadal Ocean Temperature and Salinity Variability in the Tropical North Atlantic: Linking with the AMO, AMOC, and Subtropical Cell, *J. Climate*, 26(16): 6137–6162, <https://doi.org/10.1175/JCLI-D-12-00721.1>, 2013.
- Zeeberg, J., Corten, A., Tjoe-Awie, P., Coca, J., and Hamady, B.: Climate modulates the effects of *Sardinella aurita* fisheries off Northwest Africa, *Fish. Res.*, 89, 65–75, 2008.
- 747 Zenk, W., Klein, B., and Schröder, M.: Cape Verde Frontal Zone, *Deep-Sea Res.*, 38, S505–S530, 1991.

750

753

756

Captions

TABLES

759 Table 1: Data deployment at site CBmeso (=Cape Blanc mesotrophic): trap name, coordinates (latitude and longitude), ocean bottom depth, trap depth, sampling interval and sample amount.

Table 1 Romero et al.

Trap name	LAT		Bottom depth m	Trap depth m	Sampling		nr. of samples	Previously published by
	N	W			start	end		
CBmeso1 lower	20°45.3'	19°44.5'	3646	2195	03/22/88	03/08/89	13	Lange et al. (1998), Romero et al. (2002)
CBmeso2 lower	21°08.7'	20°41.2'	4092	3502	03/15/89	03/24/90	22	Romero et al. (2002)
CBmeso3 lower	21°08.3'	20°40.3'	4094	3557	04/29/90	04/08/91	17	Romero et al. (2002)
CBmeso4 lower	21°08.7'	20°41.2'	4108	3562	03/03/91	11/19/91	13	Romero et al. (2002)
CBmeso5 lower	21°08.6'	20°40.9'	4119	3587	06/06/94	08/27/94	19	
<i>CBmeso6 upper*</i>	21°15.0'	20°41.8'	4137	771	09/02/94	10/16/94	2	
CBmeso7 lower	21°15.4'	20°41.8'	4152	3586	11/20/95	01/29/97	20	
<i>CBmeso8 upper*</i>	21°16.3'	20°41.5'	4120	745	01/30/97	06/04/98	8	
CBmeso9 lower	21°15.2'	20°42.4'	4121	3580	11/06/98	07/11/99	20	
CBmeso12 lower*	21°16.0'	20°46.5'	4145	3610	04/05/01	12/17/01	14	
CBmeso13 lower	21°16.8'	20°46.7'	4131	3606	04/23/02	05/08/03	20	
<i>CBmeso14 upper</i>	21°17.2'	20°47.6'	4162	1246	05/31/03	04/18/04	10	
CBmeso15 lower	21°17.9'	20°47.8'	4162	3624	04/17/04	07/21/05	20	
CBmeso16 lower	21°16.8'	20°47.8'	4160	3633	07/25/05	09/28/06	20	
CBmeso17 lower	21°16.4'	20°48.2'	4152	3614	10/24/06	25.03.07	20	
CBmeso18 lower	21°16.9'	20°48.1'	4168	3629	03/25/07	04/05/08	20	
CBmeso19 lower	21°16.2'	20°48.7'	4155	3617	04/22/08	03/22/09	20	
CBmeso20 lower*	21°15.6'	20°50.7'	4170	3620	04/03/09	05/25/09	4	

Asterisks represent traps with malfunctioning, leaving gaps in the diatom record.

762

765

768

771

Table 2: Species composition of the assemblage of diatoms at site CBmeso between March 1988 and June 2009.

Group	Species	Main References
1) Benthic	<i>Actinoptychus senarius</i> <i>Actinoptychus vulgaris</i> <i>Biddulphia alternans</i> <i>Cocconeis</i> spp. <i>Delphineis surirella</i> <i>Diploneis</i> spp. <i>Gomphonema</i> spp. <i>Odontella mobiliensis</i> <i>Paralia sulcata</i> <i>Psammodyction panduriformis</i> <i>Rhaphoneris amphiceros</i> <i>Tryblionella</i> spp.	Andrews (1981), Round et al. (1990), Hasle and Syvertsen (1996).
2) Coastal upwelling	<i>Chaetoceros affinis</i> <i>Chaetoceros cinctus</i> <i>Chaetoceros compressus</i> <i>Chaetoceros constrictus</i> <i>Chaetoceros coronatus</i> <i>Chaetoceros debilis</i> <i>Chaetoceros diadema</i> <i>Chaetoceros radicans</i> <i>Thalassionema nitzschioides</i> var. <i>nitzschioides</i>	Hasle and Syvertsen (1996); Abrantes et al. (2002); Nave et al., 2001; Romero et al., 2002; Romero and Armand, 2010)
3) Coastal planktonic	<i>Actinocyclus curvatus</i> <i>Actinocyclus octonarius</i> <i>Actinocyclus subtilis</i> <i>Azpeitia barronii</i> <i>Chaetoceros concavicornis</i> (vegetative cell) <i>Coscinodiscus argus</i> <i>Coscinodiscus centralis</i> <i>Coscinodiscus radiatus</i> <i>Cyclotella litoralis</i> <i>Proboscia alata</i> <i>Shionodiscus oestrupii</i> var. <i>venrickae</i> <i>Stellarima stellaris</i> <i>Thalassionema pseudonitzschioides</i> <i>Thalassiosira binata</i> <i>Thalassiosira conferta</i> <i>Thalassiosira delicatula</i> <i>Thalassiosira dyporocycus</i> <i>Thalassiosira elsayedii</i> <i>Thalassiosira poro-irregulata</i>	Romero and Armand (2010), Romero and Fischer (2017); Crosta et al. (2012); Romero et al. (2009, 2012, 2020)



	<i>Thalassiosira rotula</i>	
4) Open-ocean	<i>Alveus marinus</i>	Romero and Armand (2010), Romero and Fischer (2017), Romero et al. (2005), Crosta et al. (2012), Romero et al. (2020).
	<i>Aserolampra marylandica</i>	
	<i>Asteromphalus arachne</i>	
	<i>Asteromphalus cleveanus</i>	
	<i>Asteromphalus flabellatus</i>	
	<i>Asteromphalus heptactis</i>	
	<i>Asteromphalus sarcophagus</i>	
	<i>Azpetia africana</i>	
	<i>Azpetia neocrenulata</i>	
	<i>Azpetia nodulifera</i>	
	<i>Azpetia tabularis</i>	
	<i>Bacteriastrum elongatum</i>	
	<i>Bogorovia</i> spp.	
	<i>Coscinodiscus reniformis</i>	
	<i>Detonula pumila</i>	
	<i>Fragilariopsis doliolus</i>	
	<i>Guinardia cyclindrus</i>	
	<i>Haslea</i> spp.	
	<i>Hemidiscus cuneiformis</i>	
	<i>Leptocyclindrus mediterraneus</i>	
	<i>Nitzschia aequatoriale</i>	
	<i>Nitzschia bicapitata</i>	
	<i>Nitzschia capuluspalae</i>	
	<i>Nitzschia interruptestriata</i>	
	<i>Nitzschia sicula</i>	
	<i>Nitzschia sicula</i> var. <i>rostrata</i>	
	<i>Planktoniella sol</i>	
	<i>Pseudo-nitzschia</i> spp.	
	<i>Pseudosolenia calcar-avis</i>	
	<i>Pseudotriceratium punctatum</i>	
	<i>Rhizosolenia acuminata</i>	
	<i>Rhizosolenia bergonii</i>	
	<i>Rhizosolenia imbricatae</i>	
	<i>Rhizosolenia robusta</i>	
	<i>Rhizosolenia setigera</i>	
	<i>Rhizosolenia styliformis</i>	
	<i>Roperia tessellata</i>	
	<i>Shionodiscus oestrupii</i> var. <i>oestrupii</i>	
	<i>Thalassionema bacillare</i>	
	<i>Thalassionema frauenfeldii</i>	
	<i>Thalassionema nitzschioides</i> var. <i>capitulata</i>	
	<i>Thalassionema nitzschioides</i> var. <i>inflata</i>	
	<i>Thalassionema nitzschioides</i> var. <i>lanceolata</i>	
	<i>Thalassionema nitzschioides</i> var. <i>parva</i>	
	<i>Thalassiosira eccentrica</i>	
	<i>Thalassiosira endoseriata</i>	
	<i>Thalassiosira ferelineata</i>	
	<i>Thalassiosira lentiginosa</i>	
	<i>Thalassiosira leptopus</i>	
	<i>Thalassiosira lineata</i>	
	<i>Thalassiosira nanolineata</i>	



Thalassiosira parthenia
Thalassiosira plicata
Thalassiosira punctigera
Thalassiosira sacketii var. *sacketii*
Thalassiosira sacketii var. *plana*
Thalassiosira subtilis
Thalassiosira symmetrica
Thalassiothrix spp.

774

777

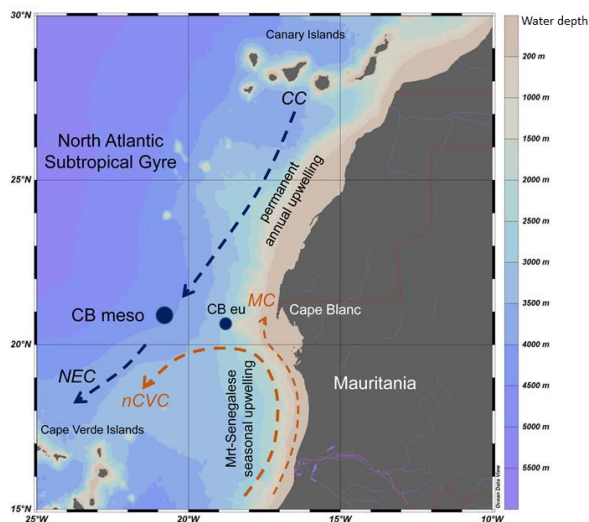
780

783

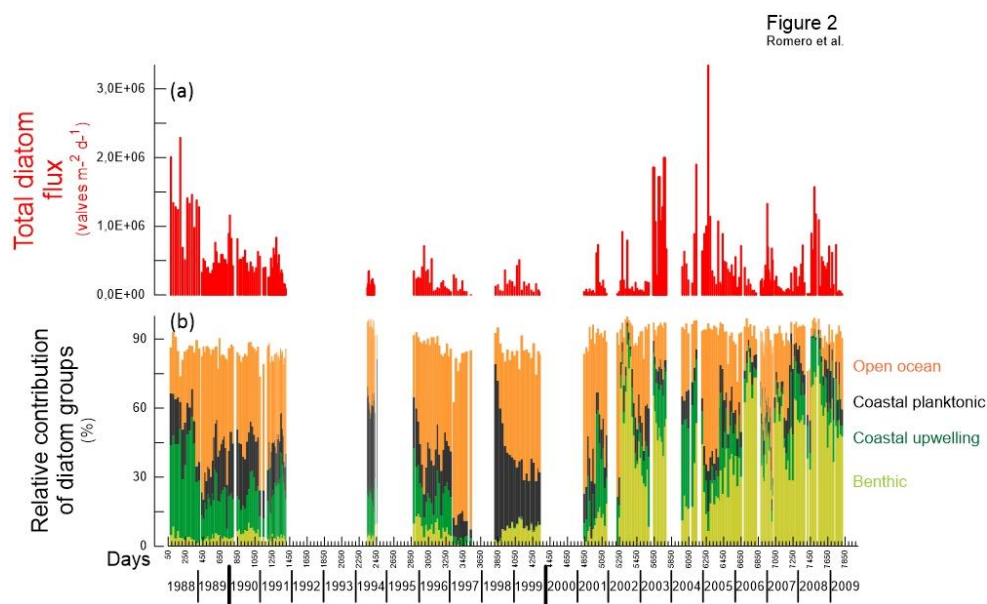
786

789 FIGURES

Figure 1
Romero et al.



792 Figure 1. Map of the study area showing the locations of the sediment trap sites CBmeso and CBeu
795 (dark blue dots). Major surface currents are also shown (Canary Current=CC; Mauritanian
Current=MC; North Equatorial Current (NEC), north Cape Verde Current=nCVC). The upwelling
zones along the northwestern African margin are depicted after Cropper et al. (2014). The color
scale (right-hand side) refers to meters below surface water (0 m).



798

Figure 2. Total diatom flux (valves m⁻² d⁻¹) and relative contribution of diatom groups (relative contribution, %) for the interval March 1998 and June 2009 at the CBmeso site. Groups of diatoms are: benthic (light green), coastal planktonic (black), coastal upwelling (dark green), and open-ocean (orange). For the species-specific composition of each group see 4.2. and Table 2. For interpretation of the references to color in this figure legend, the reader is referred to the web version of this article.

807

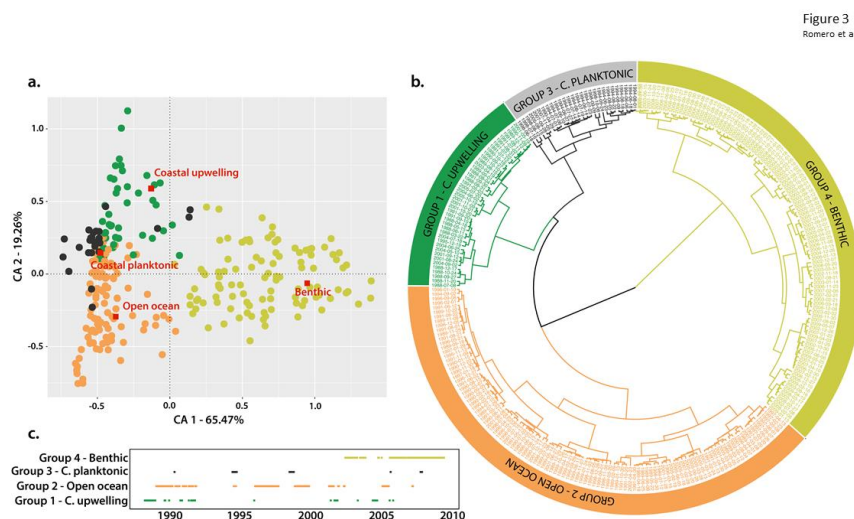


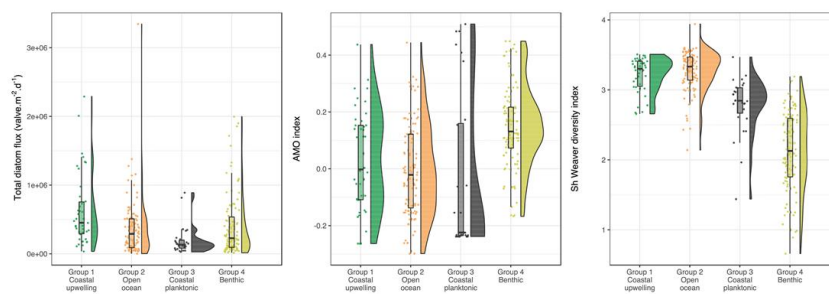
Figure 3
Romero et al.

810

813 Figure 3. (a) Correspondence Analysis (CA) of diatom groups found at CBmeso site between March
1988 and June 2009, coupled with (b) a hierarchical clustering analysis of samples' score resulting
from CA (see 2.3 Statistical analysis). Note that in 3a the red squares for each group represents the
816 centroid of dates and their placement within the corresponding group. The corresponding group's
name is written in red. (c) The time series of the four diatom groups identified by both multivariate
analysis (CA and clustering) is also represented. Colours used for identifying each diatom group are
819 the same as in Fig. 2b. Euclidean distance and Ward's aggregation link were used to perform the
hierarchical dendrogram. For the species-specific composition of each group see 4.2. and Table 2.
For interpretation of the references to colour in this figure legend, the reader is referred to the web
822 version of this article.



Figure 4
Romero et al.



825 Figure 4: Comparison of (a) clusters extracted from multivariate analysis with the environmental
826 forcing variables (a1: Total diatom flux; a2: AMO; a3: Shannon diversity). Colours used for
827 identifying each diatom group are the same as in Fig. 2b.

828

831

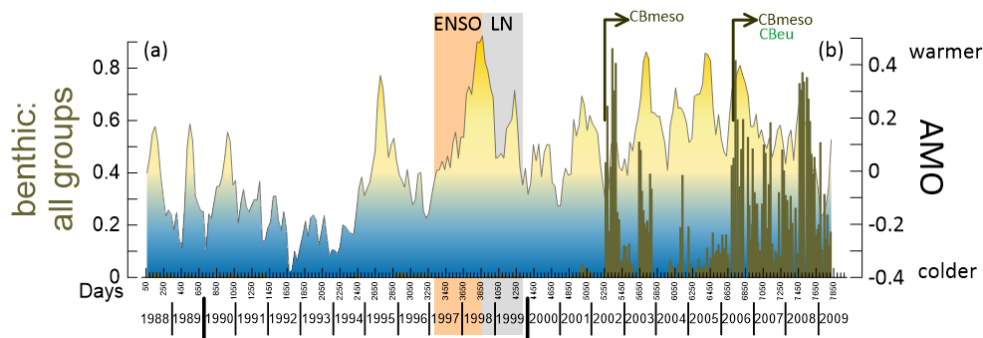
834

837



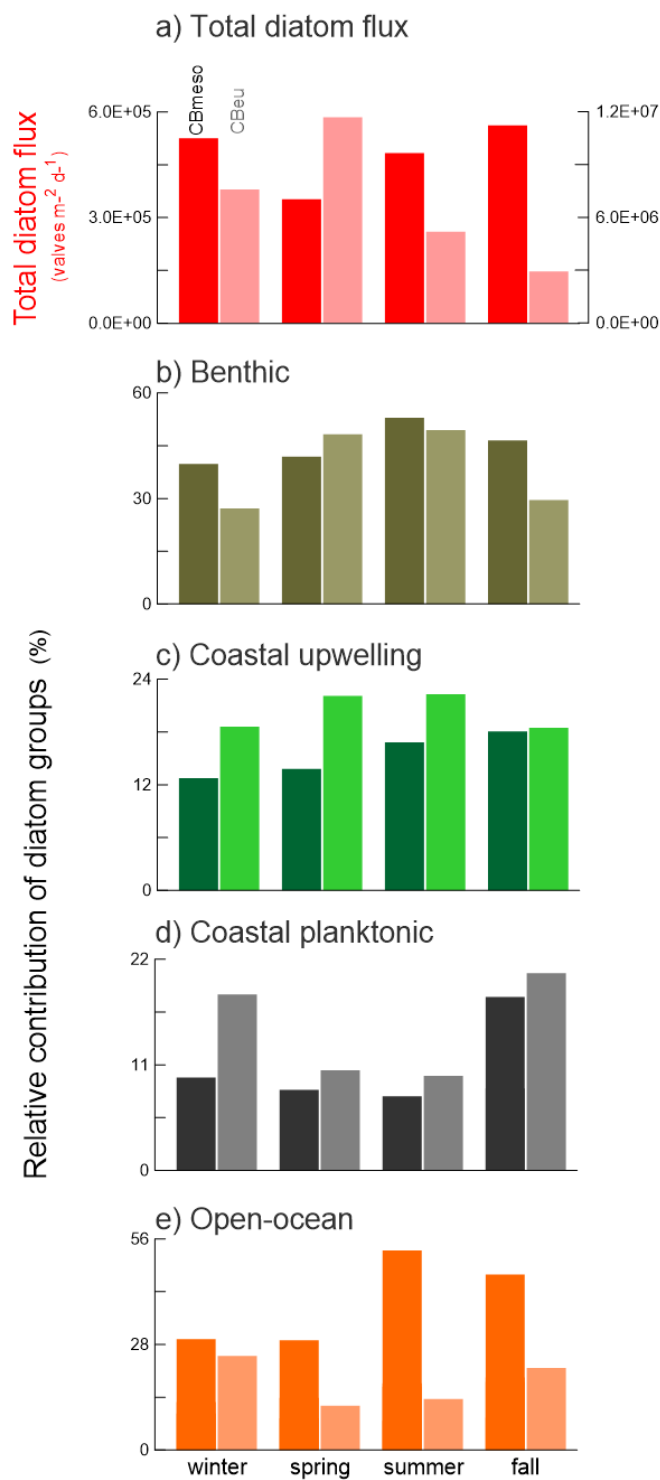
840

Figure 5
Romero et al.



843 Figure 5: Time-series of ratio benthic:all groups (olive bars, a) at site CBmeso and the Atlantic
Multidecadal Oscillation (AMO, b) between March 1988 and May 2009. The fill in (b) represents the
colder phase (blue) and the warmer phase (yellow) of AMO. Inverted arrows in the lower panel
846 below the benthic:all groups bars represent the abrupt increase of relative contribution of benthic
diatoms, first seen at CBmeso in early winter 2002 and in winter 2006 at CBmeso and at CBeu
(Romero and Fischer, 2017; Romero et al., 2020). Shadings in the background: light orange, El
849 Niño/Southern Oscillation (ENSO); grey, La Niña (LN). For interpretation of the references to color
in this figure legend, the reader is referred to the web version of this article.

Figure 6
 Romero et al.





855 Figure 6: Comparison of seasonal values of (a) total diatom flux (valves $\text{m}^{-2} \text{d}^{-1}$) and (b-e) the relative
contribution of diatom groups (%) at sites CBmeso and CBeu (see 2.1 for trap locations). Darker
858 colors represent flux and relative percentage at CBmeso, while lighter those of CBeu. Note that the
right y-axis for (a) total diatom flux correspond to CBeu and the left-hand y-axis to the CBmeso site.
For the species-specific composition of each group at CBmeso see 4.2. and Table 2. The species-
specific composition of groups at CBeu is originally published in Romero and Fischer (2017). Colours
used for identifying each diatom group are the same as in Fig. 2b. For interpretation of the
references to color in this figure legend, the reader is referred to the web version of this article.